Research Article

Received: 26 August 2014 Revised: 7 December 2014 Accepted article published: 15 December 2014 Published online in Wiley Online Library:

(wileyonlinelibrary.com) DOI 10.1002/pi.4851

Molecularly imprinted hydrogels from colloidal crystals for the detection of progesterone

Natalia Casis,[a] Carlos Busatto,[a] María M Fidalgo de Cortalezzi,[b] Serge Ravaine[c] and Diana A Estenoz[a*]

Abstract

The synthesis of new nanoporous materials based on molecularly imprinted polymers (MIPs) is investigated. The novel procedure combines the non-covalent imprinting method with the colloidal crystal template technique to produce membranes with pre-specified morphology capable of selectively recognizing progesterone. The colloidal crystals made of silica particles were obtained by Langmuir – Blodgett and self-assembly techniques, and exhibited a considerable control of the film thickness. Hydrogel films were prepared by copolymerization of acrylic acid and ethylene glycol dimethacrylate in the presence of 2,2′-azobisisobutyronitrile as initiator. The polymerization took place in the interspaces of the colloidal crystal and after the reaction was finished the silica particles were etched with hydrofluoric acid to produce a 3D ordered structure. The nanocavities derived from progesterone were distributed within the walls of the internal structure of the films. The equilibrium swelling properties of the MIPs were studied as a function of crosslinking degree and pH. The pore morphology of the film was analyzed by SEM. The MIP characterizations were accomplished by several techniques, e.g. Fourier transform infrared spectroscopy, DSC and evaluation of their sensing and selective properties.

Keywords: hydrogels; colloidal crystals; water treatment; imprinted polymer

INTRODUCTION

Emerging contaminants derived from the pharmaceutical family such as endocrine disruptors are being found with increasing frequency in wastewater.[1,2] This concern stimulates the development of new selective analytical methods for their detection.[3,4] Steroid hormones (such as progesterone, testosterone, estradiol and others) are released into surface waters in large amounts and generate adverse biological effects on health. Exposure to environmental estrogens has been shown to decrease sperm count, increase rates of testicular, prostate and breast cancer, and produce reproductive disorders in human males.[5–7] Conventionally methods to detect organic compounds involve not only expensive instrumentation but also a large number of separating analytical procedures, resulting in a complex, time consuming and laborious screening procedure. For this reason, the development of novel approaches for easy and rapid drug detection is highly desirable. Molecular imprinting is a well established technique used to synthesize molecularly imprinted polymers (MIPs) with specific molecular recognition nanocavities.[8] Owing to the complementarity in shape and binding sites, the created nanocavities exhibit high selectivity towards the imprinted molecules, including a large and diverse set of important organic compounds, e.g. hormones, or metal ions.[9–11]

Recently, researchers have proposed an original procedure that combines molecular imprinting and colloidal crystals to prepare polymers with 3D, highly ordered, macroporous structures and specific binding nanocavities for a rapid assay to detect organic compounds like bisphenol A,[12,13] atrazine in aqueous solution[14] and specific stimulants like theophylline or ephedrine in urinous buffer.[15] The high sensitivity and specificity observed in these polymeric systems is mainly due to the high surface-to-volume ratios of the structure that allow for a more efficient mass transport in submicrometer-sized pores and enhance surface reactions. In particular, highly ordered porous materials based on hydrogels are able to swell or shrink in aqueous solution upon molecular recognition or environmental conditions leading to a change in optical properties.[16–19] The highly controlled pore structure achieved through the colloidal template technique is especially beneficial in sensor applications, since it gives elevated specific surface areas, more interaction sites, efficient mass transport, easier accessibility to the active sites through the interconnected macroporous system, as well as high specificity to analytes of the nanocavities.[20,21] Despite the excellent results and advantages of these systems for the detection of organic compounds, studies on their applications for hormone detection have not been reported yet.

The determination of hormones in complex matrices like wastewater requires appropriate isolation and preconcentration

* *Correspondence to: Diana A. Estenoz, Instituto de Desarrollo Tecnológico para la Industria Química, INTEC (Universidad Nacional del Litoral and CONICET), Güemes 3450, 3000 Santa Fe, Argentina.*
E-mail: destenoz@santafe-conicet.gov.ar

a *Instituto de Desarrollo Tecnológico para la Industria Química INTEC (Universidad Nacional del Litoral and CONICET), Güemes 3450, 3000, Santa Fe, Argentina*

b *Department of Civil and Environmental Engineering, University of Missouri, Columbia, Missouri 65211, USA*

c *Centre de Recherche Paul Pascal – CNRS, 115 avenue du Dr Schweitzer, 33600 Pessac, France*

Table 1. Mixture composition for the synthesis of MIPs

	AA (mL)	EGDMA (mL)	AA:EGDMA (molar ratio)	Progesterone (mg)	Ethanol (mL)	AIBN (mg)
P1	0.80	0.02	1:0.01	4.0	0.6	2.0
P2	0.80	0.04	1:0.02	4.0	0.6	2.0
P3	0.80	0.06	1:0.03	4.0	0.6	2.0
P4	0.80	0.2	1:0.1	4.0	0.6	2.0
P5	0.80	0.55	1:0.25	5.42	0.6	2.0
P6	0.80	1.10	1:0.5	6.94	0.6	2.0

methods that often lack reproducibility and sensitivity.[22] HPLC coupled with detectors such as spectroscopic ultraviolet – visible (UV – visible), diode array, fluorescence and mass spectroscopy offers the most accurate and effective tool for the determination of progesterone up to a limit of detection of 0.04 – 2.01 ng L^{-1} in environmental waters, 0.08 – 2.84 ng g^{-1} in soils, 26 – 175 ng g^{-1} in sewage sludge and 140 – 410 ng L^{-1} in wastewater.[23] The variations in the limits of detection with samples and extraction methods hints to the importance of the preconcentration and extraction steps, making the overall process time consuming and susceptible to errors.

In the present work, thin films were synthesized based on hydrogels by combination of the non-covalent imprinting method and the colloidal crystal template procedure. The fabricated films were tested for the detection of progesterone in water.

EXPERIMENTAL

Materials

Tetraethoxysilane (TEOS) (Fluka, Seelze, Germany), ammonia solution (25% in water, Merck, Dermastadt, Germany), ethanol (J. T. Baker, Center Valley, PA, USA), ethylene glycol dimethacrylate (EGDMA) (98%, Merck, Hohenbrunn, Germany), 2,2′-azobisisobutyronitrile (AIBN) (98%, Sigma-Aldrich, St. Louis, MO, USA), progesterone and 17β-estradiol (99%, Sigma-Aldrich, St. Louis, MO, USA), hydrofluoric acid (49%, Fisher, Fair Lawn, NJ, USA), acetic acid (96%, Merck, Hohenbrunn, Germany) and phosphate buffer solution (Fisher, Fair Lawn, NJ, USA) were purchased at reagent grade and used without further purification. Acrylic acid (AA) (99%, Merck, Hohenbrunn, Germany) was vacuum distilled at 50 °C and 25 mmHg prior to use to remove the inhibitor hydroquinone.

Synthesis of the colloidal crystal template and hydrogel films

The synthesis of silica particles and colloidal crystals was carried out following the procedure described in a previous work.[24] Briefly, the monodisperse silica particles were synthesized by an approach based on the Stöber method.[25] TEOS (11 mL) and ethanol (210 mL) were mixed in a flask and stirred. Then, ammonia (11 mL) and deionized water (17 mL) were introduced and allowed to react for 4 h. An additional 11 mL TEOS and 10 mL water were added to the flask and the solution was again stirred for 4 h to allow further reaction. The silica particles obtained were centrifuged and redispersed in ethanol three times to completely wash the particles. A cleaned glass slide was vertically placed into a flask containing silica particles suspended in ethanol and, after volatilization of the solvent, colloidal crystals were formed on both sides of the slide. For the formulation of MIPs, mixtures were prepared from AA as the functional monomer, EGDMA as the crosslinker agent, AIBN as the initiator, progesterone as the target molecule and ethanol as solvent. Different molar ratios of AA:EGDMA were used for fabrication of the MIPs (Table 1). The steps in the film fabrication are shown in Fig. 1. The homogeneous mixture was added dropwise on a silica colloidal crystal deposited on a glass slide. Another slide was placed upon the colloidal crystal film and the two slides were held together to retain the above-mentioned precursor mixture, forming a 'sandwich' structure (Fig. 1(a)).

Polymerization was performed under UV light at 365 nm for 3 h (Cole Parmer lamp, $I = 2$ mW cm^{-2}) at $T = 25$ °C. Then, the silica particles were removed by immersing the system for 12 h in 5% hydrofluoric acid solution. Finally, to remove progesterone, the resulting polymer film was immersed in a 0.1 mol L^{-1} acetic acid solution for 2 h (Fig. 1(b)). To check the extraction efficiency process of target molecule from the matrix, the resulting washing solution was analyzed by HPLC until it evidenced the absence of progesterone. The films obtained were further rinsed with ethanol to remove the remaining acetic acid. The non-imprinted polymer (NIP) was prepared using the same procedure but with no addition of progesterone.

Characterization

Size and morphology

Silica particles and porous films were imaged by SEM using a JEOL JSM-840A and JEOL JSM 35C to analyze the pore size and morphology. Samples were attached to a metal mount using carbon tape and were coated with a thin layer of gold to provide a conductive surface using a sputter coater (CRC-100). Quantitative analysis of the images was completed using ImageJ software (National Institutes of Health).

The particle size distribution of the synthesized silica particles was determined by dynamic light scattering (DLS) using a Malvern Nanosizer 2000.

Thermal analyses

The thermal properties of the fabricated films were determined by the DSC technique. The analyses were performed in a DSC Mettler TA 300. The samples (2 – 5 mg of a lyophilized hydrogel) were sealed into DSC aluminium pans. An empty aluminium pan was used as reference material. The samples were studied at heating rates of 10 °C min^{-1} between −50 °C and 150 °C and between −50 °C and 300 °C.

Equilibrium swelling properties

Swelling experiments were performed on MIPs and NIPs in phosphate buffer at three different pH values (4, 7 and 10) at 25 °C. The polymers were swollen in solutions for 72 h at ambient temperature to reach equilibrium and the degree of swelling was determined gravimetrically. The percentage swelling ratio (SR) was calculated from the expression

$$\%\ \mathrm{SR} = \left(m_s - m_d\right)/m_d \quad (1)$$

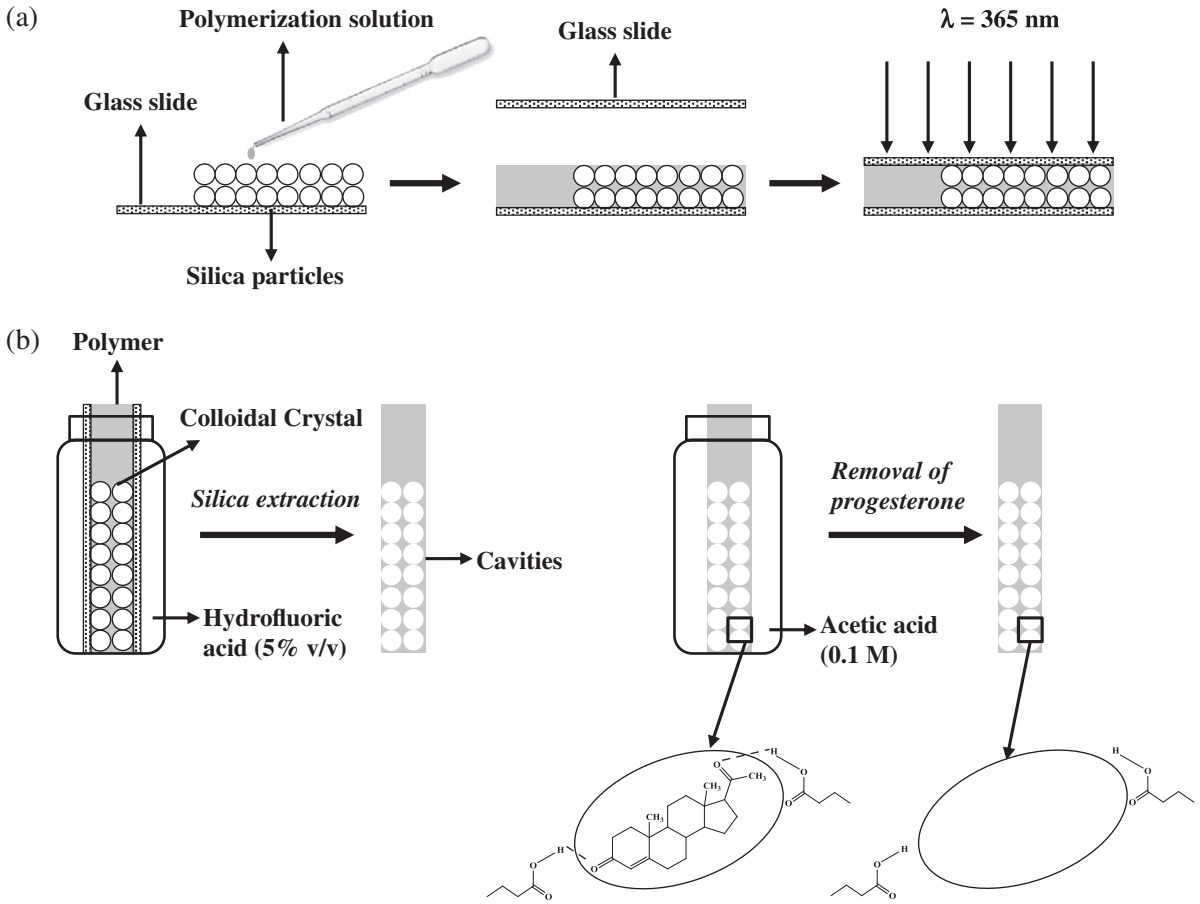

Figure 1. (a) Infiltration and polymerization process. (b) Silica extraction and removal of progesterone.

where m_s is the mass of the swollen film at equilibrium and m_d is the mass of the freeze dried films.

Fourier transform infrared spectroscopy (FTIR)

FTIR was used to determine the polymer structures and evaluate the interaction between membranes and progesterone. The infrared spectra of dried MIPs were obtained by preparing KBr pellets in a Perkin-Elmer Spectrum One-FTIR.

Evaluation of MIPs

Recognition properties of MIPs

Recognition studies were conducted by weighing approximately 4 – 6 mg of dried (MIPs and NIPs) films and immersing them in a progesterone solution of known concentration (5 ppm) until equilibrium was reached (i.e. 24 h later). The residual concentrations of the progesterone solutions were determined by HPLC in a Waters 1525 HPLC system with a DA detector. The column used was an XbridgeTM C18 (150 mm × 4.6 mm; particle size 5 µm; Waters). The flow rate was 1 mL min^{-1} and an isocratic elution of methanol – water (90:10% v/v) was used. The recognition capacity (RC) is defined as the adsorbate mass per unit of adsorbent mass and is calculated from the equation

$$RC = (C_i - C_e)\,Vt/m \quad (2)$$

where C_i and C_e are the initial and the equilibrium concentrations of the adsorbate in solution (in mg mL^{-1}), respectively, Vt is the volume of solution (in mL) and m is the mass of the xerogel (in g). Then, the imprinting polymer efficiency (IE) is defined by

$$IE = RC_{MIP}/RC_{NIP} \quad (3)$$

where RC_{MIP} and RC_{NIP} are the recognition capacities of MIP and NIP, respectively.

Selectivity of MIPs

Selectivity studies were carried out in a similar way to the recognition studies of progesterone, but in this assay MIPs were incubated in the presence of progesterone and 17β-estradiol, another steroid hormone frequently found as a contaminant in water, in an equal molar concentration of 0.05 mol L^{-1}. The hormone 17β-estradiol was chosen for the selectivity analyses because it presents a very similar structure to the progesterone molecule (Fig. 2). For the detection, conventional chromatographic separations were performed with a dual λ absorbance detector ($\lambda = 245$ nm for progesterone and $\lambda = 280$ nm for 17β-estradiol).

All selectivity and recognition studies were carried out in duplicate.

RESULTS AND DISCUSSION

Silica particles of narrow size distributions were obtained through strict control of the synthesis parameters. This property is essential for obtaining a well organized deposit that will lead, in turn, to a fully interconnected pore structure in the films. The particle

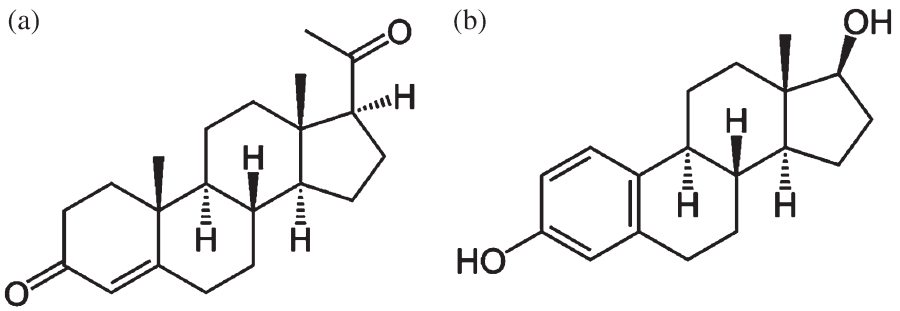

Figure 2. Chemical structures of (a) progesterone and (b) 17β-estradiol.

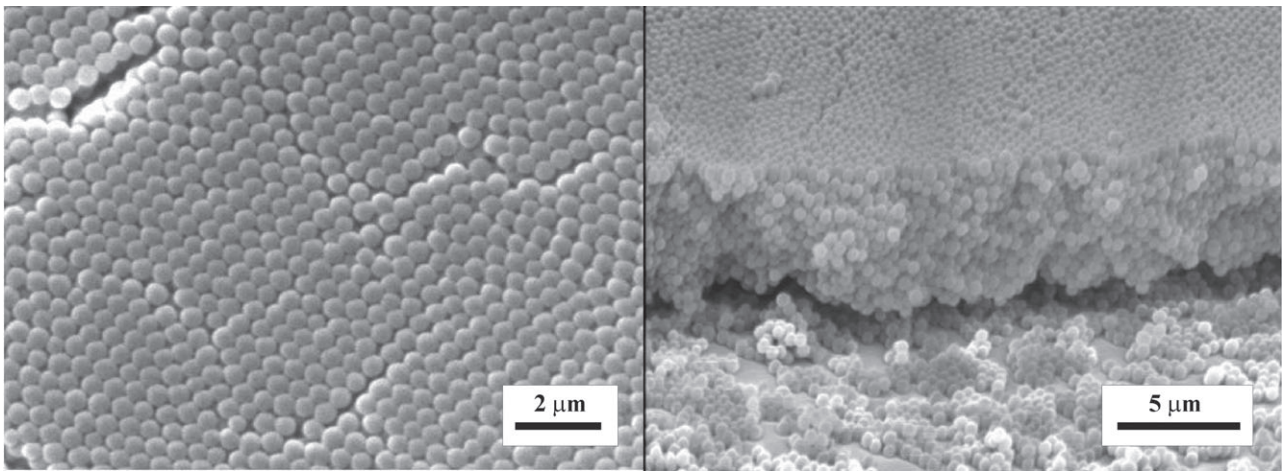

Figure 3. Colloidal crystal: (a) top view; (b) cross-sectional view.

sizes obtained by DLS and SEM (575 ± 12 nm and 573 ± 29 nm, respectively) showed good agreement between results from the two techniques.

SEM images of particle templates are shown in Fig. 3. The thickness of the self-assembled deposits can be controlled by changing the volume fraction of the initial particle suspension.[26] For a 1.2% initial volume fraction, approximately 20 layers of silica particles were obtained (Fig. 3(b)) as determined by SEM. Based on this measurement, the thickness of the films is expected to be approximately 10 μm.

A photograph of the porous films as well as SEM micrographs are shown in Fig. 4. The surface porosity is illustrated in Fig. 4(a). The images correspond to the P4 sample, but this is representative of all films since target molecule concentration is not expected to affect the pore morphology. The internal porous structure presents cavities having a similar size to the silica particles used to create the template (Fig. 4(b)). The effective, i.e. connective, pores correspond to the openings that link the cavities and arise from the contact points of particles in the deposit; their size was determined to be 93 ± 8 nm.

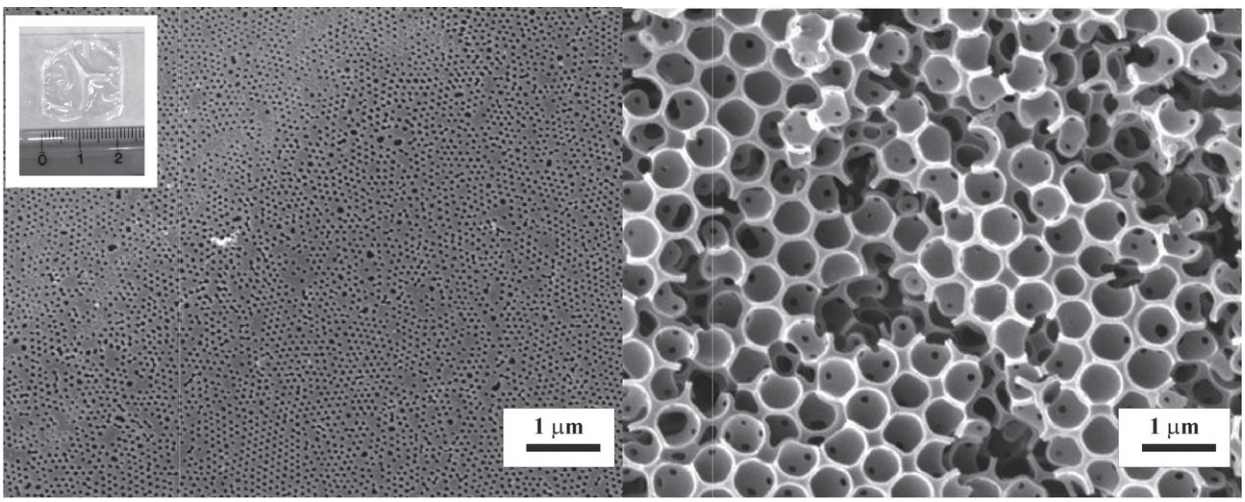

Figure 4. Nanoporous imprinted film: (a) photograph and SEM micrograph of the top view showing surface porosity and (b) internal porosity.

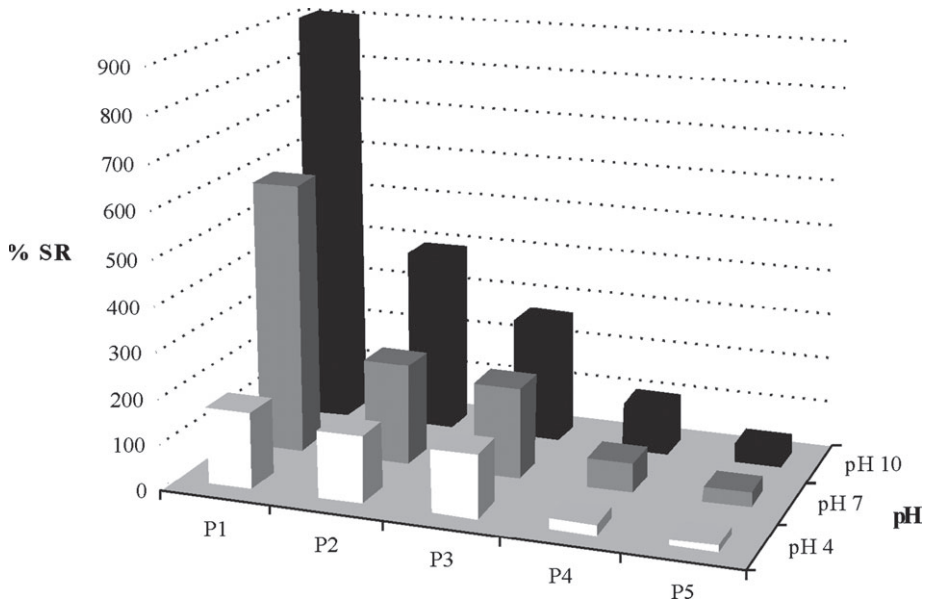

Figure 5. Swelling ratio (%) of MIPs at pH 4, 7 and 10.

Table 2. Transition temperatures (T_g) of MIPs

	T_g (°C)
P1	38
P2	40
P3	45.5
P4	56.5
P5	62.5
P6	67.5

The swelling ratio was investigated as it can be considered an indirect measurement of crosslinking, which affects the efficiency and specificity of the MIPs. Figure 5 shows the percentage swelling ratio in deionized water as a function of pH for MIPs 1 – 5. All samples exhibit a high value indicating a high water absorption capacity. With higher crosslinking degree, a decrease of the polymer chain mobility and an increase in the hydrophobicity of the polymeric network due to a higher content of the hydrophobic crosslinker is expected. As a result of these effects, the swelling is reduced at each pH value due to the hindering of water diffusion within the film. On the other hand, for all samples, increases of the swelling ratio at higher pH values were observed. At low pH values, carboxyl groups present in the polymer reduce the repulsive interactions between the polymer chains, resulting in less swelling. In contrast, at neutral and alkaline pH values when carboxyl groups become deprotonated, electrostatic repulsion together with the breaking of hydrogen bonds generate an increase of the material swelling.

Another property related to crosslinking degree is the glass transition temperature (T_g). DSC analysis were performed for all polymers in the dried state, and the results are presented in Table 2. As expected, T_g increases with the percentage of crosslinking. Also, for all samples, the degradation process starts at approximately 195 °C.

In order to evaluate the capability of the films to capture the progesterone molecule, two independent techniques were applied: FTIR, as a qualitative measurement of target molecule – film interaction; and HPLC, to quantitatively estimate the capture efficiency. Figure 6 shows the FTIR spectra of P4 MIP in the presence and absence of progesterone, i.e. before and after the progesterone incubation. The O – H group band allows for the detection of hydrogen bonds. The hydroxyl groups in the carboxylic acids can

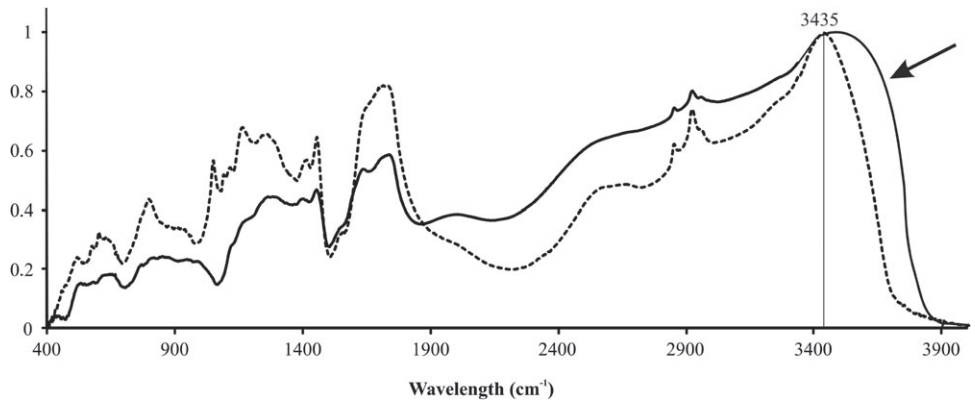

Figure 6. FTIR spectra of MIP before and after progesterone removal.

Table 3. Recognition studies of MIPs and NIPs

	Recognition studies	
	RC (mg g^{-1}) MIPs	IE
P1	2.02	1.43
P2	2.21	1.65
P3	2.43	1.89
P4	2.85	3.15
P5	2.32	2.28
P6	2.38	2.49

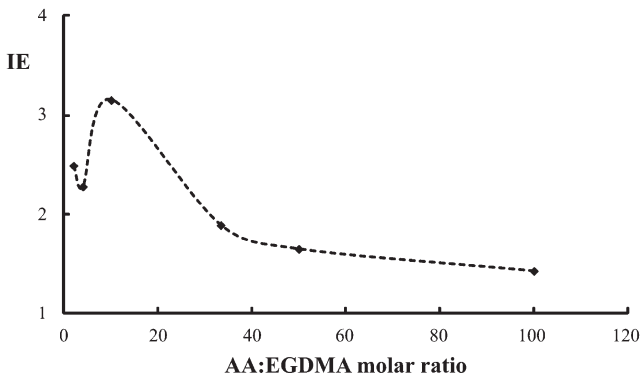

Figure 7. Imprinting efficiency: IE *versus* AA:EGDMA molar ratio.

be observed at 3435 cm^{-1}. MIPs containing progesterone exhibit a widening of the O – H group band indicating the presence of hydrogen bonds.

Table 3 presents the recognition and selectivity studies of MIPs and NIPs. The results indicate a superior recognition capacity of MIPs for progesterone in comparison to NIPs with an IE from 1.43 to 3.15. Progesterone binds to the NIP films by non-specific interactions such as hydrophobic effects, whereas the MIPs, due to the presence of specific binding cavities, are able to retain a more significant percentage of drug. Such behavior is in accordance with a model of retention mechanism which assumes that the selective sites have stronger interaction with the drug than non-selective sites.[27] As shown in Fig. 7, IE initially increased with crosslinking degree, but it reached a maximum value of 3.15 for a monomer:crosslinker ratio of 1:0.2 (P4).

The observed maximum is a consequence of two opposite effects: the improved diffusion of the target molecule within the polymer at low crosslinking degree, and the stability of the template structure and the imprinted nanocavities at high crosslinking degree.

Regarding the selectivity of the MIPs, the recognition capability for progesterone decreases in the presence of 17β-estradiol due to the similarity of the structures of the two hormones. However, all values of recognition capacity are higher for progesterone than for 17β-estradiol. The specificity of the MIPs depends mainly on the shape of the target molecule and the degree of interaction of binding sites. Due to the complementary shape, size and interaction sites with the formed binding sites, progesterone preferentially occupies the imprinted cavities within the hydrogel film. Also, as the degree of crosslinking increases the selectivity is improved, as indicated by the ratio of IE(progesterone):IE(estradiol) (Table 4). This can be explained by the effect of crosslinking on swelling. As the SR decreases with a higher degree of crosslinking, there will be less deformation of the binding sites and the selectivity to the imprinted molecule is expected to improve. Furthermore, a higher crosslinker degree in the polymer formulation would lead to a more rigid structure, with a superior capacity to preserve the cavities left by the target molecule after removal from the template.

Table 4. Selectivity studies of MIPs and NIPs

	Selectivity studies				
	Progesterone		17β-estradiol		
	RC_p (mg g^{-1})	IE_p	RC_e (mg g^{-1})	IE_e	IE_p/IE_e
P1	1.52	1.43	0.51	1.32	1.08
P2	1.66	1.65	0.53	1.38	1.20
P3	1.82	1.89	0.63	1.45	1.30
P4	2.14	3.15	0.68	1.79	1.76
P5	1.74	2.28	0.62	1.27	1.80
P6	1.79	2.49	0.60	1.33	1.87

CONCLUSIONS

A new method for the synthesis of materials based on colloidal crystals and molecular imprinting techniques was studied. The materials can be used for simple, time-saving, and low cost detection and capture of progesterone.

Silica particles an average of 575 nm in diameter led to highly organized porous structures that did not show evidence of distortion by the presence of the imprinting molecule. The fabricated films exhibited high capacity to adsorb water and swell; the swelling increased with pH and was inversely related to the crosslinking degree, due to the higher hydrophobicity and rigidity of the material. The material showed thermal stability up to 195 °C.

The monomer to crosslinker ratio significantly affects the imprinting efficiency. An optimum value of 1:0.2 AA:EGDMA was identified, where imprinted efficiency was maximized.

The developed system showed good reproducibility and would allow for rapid quantification of the target molecule concentration in the photonic films through spectroscopic techniques. In future work the capability of the photonic sensing will be investigated in order to develop a new type of sensor for the detection of progesterone and other organic chemical agents. Also, the experimental work will be extended in order to study the selectivity in the presence of other analogue molecules such as testosterone and to evaluate the potential reuse from adsorption/desorption studies between drug and matrix.

ACKNOWLEDGEMENTS

Thanks to CONICET, SeCyT and Universidad Nacional del Litoral (Argentina) for financial support.

REFERENCES

1 Hecker M, Tyler CR, Hoffmann M, Maddix S and Karbe L, *Environ Sci Technol* **36**: 2311–2321 (2002).
2 Johnson AC and Sumpter JP, *Environ Sci Technol* **35**: 4697–4703 (2001).
3 Mattiessen P and Johnson I, *Environ Pollut* **146**: 9–18 (2006).
4 Auriol M, Filali-Meknassib Y, Tyagia RD, Adamsc CD and Surampallib RY, *Process Biochem* **41**: 525–539 (2006).
5 Colborn T, Vom Saal FS and Soto AM, *Environ Health Perspect* **101**: 378–384 (1993).

6 Ingerslev FH and Halling-Sorensen B, *Work Rep* **44**: 1–69 (2003).
7 Tashiro Y, Takemura A, Fujii H, Takahira K and Nakanishi Y, *Mar Pollut Bull* **47**: 143–147 (2003).
8 Caykara TC, Bozkaya U and Lu O, *J Polym Sci B Polym Phys* **41**: 1656–1664 (2003).
9 Zhu L, Chen L and Xu L, *Anal Chem* **75**: 6381–6387 (2003).
10 Wei S, Molinelli A and Mizaikoff B, *Biosens Bioelectron* **21**: 1943–1951 (2006).
11 Chen L, Xua S and Li J, *Chem Soc Rev* **40**: 2922–2942 (2011).
12 Griffete N, Frederich H, Maitre A, Cheimi MM, Ravaine S and Mangeney C, *J Mater Chem* **21**: 13052–13055 (2011).
13 Griffete N, Frederich H, Maitre A, Schwob C, Ravaine S, Carbonnier B *et al.*, *J Colloid Interface Sci* **364**: 18–23 (2011).
14 Wu Z, Tao C, Lin C, Shen D and Li G, *Chem Eur J* **14**: 11358–11368 (2008).
15 Hu X, Huang J, Zhang W, Li M, Tao C and Li G, *Adv Mater* **20**: 4074–4078 (2008).
16 Hu X, Li G, Li M, Huang J, Li Y, Gao Y *et al.*, s*Adv Funct Mater* **18**: 575–583 (2008).
17 Lee YJ and Braun PV, *Adv Mater* **15**: 563–566 (2003).
18 Hu X, An Q, Li G, Tao S and Liu J, *Angew Chem* **45**: 8145–8148 (2006).
19 Jiang P, *Angew Chem* **116**: 1554–1557 (2004).
20 Holtz JH and Asher SA, *Nature* **389**: 829–832 (1999).
21 Sharma AC, Jana T, Kesavamoorthy R, Shi L, Virji MA, Finegold DN *et al.*, *J Am Chem Soc* **126**: 2971–2977 (2004).
22 Ričanyová J, Gadzala-Kopciuch R, Reiffova K, Bazel Y and Buszewski B, *Adsorption* **16**: 473–483 (2010).
23 Tomsikova H, Aufartova J, Solich P, Sosa-Ferrera Z, Santana-Rodriguez J and Novakova L, *Trends Anal Chem* **34**: 35–58 (2012).
24 Casis N, Ravaine S, Reculusa S, Colvin VL, Wiesner MR, Estenoz DA *et al.*, *Macromol React Eng* **4**: 445–452 (2010).
25 Stöber W, Fink A and Bohn E, *J Colloid Interface Sci* **26**: 62–69 (1968).
26 Jiang P, Bertone JF, Hwang KS and Colvin VL, *Chem Mater* **11**: 2132–2140 (1999).
27 Karson JG, Andersson LI and Nicholls IA, *Anal Chim Acta* **435**: 57–64 (2001).

